



This is a repository copy of *The development and application of the stirred-reactor coupon analysis (SRCA) test method.*

White Rose Research Online URL for this paper:  
<https://eprints.whiterose.ac.uk/id/eprint/229455/>

Version: Published Version

---

**Article:**

Reiser, J.T. [orcid.org/0000-0002-2638-1580](https://orcid.org/0000-0002-2638-1580), Neeway, J.J., Cooley, S.K. et al. (26 more authors) (2025) The development and application of the stirred-reactor coupon analysis (SRCA) test method. *International Journal of Applied Glass Science*. e16707. ISSN 2041-1286

<https://doi.org/10.1111/ijag.16707>

---

**Reuse**

This article is distributed under the terms of the Creative Commons Attribution (CC BY) licence. This licence allows you to distribute, remix, tweak, and build upon the work, even commercially, as long as you credit the authors for the original work. More information and the full terms of the licence here:  
<https://creativecommons.org/licenses/>

**Takedown**

If you consider content in White Rose Research Online to be in breach of UK law, please notify us by emailing [eprints@whiterose.ac.uk](mailto:eprints@whiterose.ac.uk) including the URL of the record and the reason for the withdrawal request.



[eprints@whiterose.ac.uk](mailto:eprints@whiterose.ac.uk)  
<https://eprints.whiterose.ac.uk/>

## RESEARCH ARTICLE

# The development and application of the stirred-reactor coupon analysis (SRCA) test method

Joelle T. Reiser<sup>1</sup>  | James J. Neeway<sup>1</sup> | Scott K. Cooley<sup>1</sup> | Benjamin Parruzot<sup>1</sup>  |  
 Alejandro Heredia-Langner<sup>1</sup> | Stéphane Gin<sup>2</sup>  | Manon Thomas<sup>2</sup> |  
 Nicholas J. Smith<sup>3</sup>  | Jonathan P. Icenhower<sup>3,4</sup> | Nicholas Stone-Weiss<sup>3</sup> |  
 Yuta Takahashi<sup>5</sup> | Hajime Iwata<sup>5</sup> | Seiichiro Mitsui<sup>5</sup> | Junya Sato<sup>5</sup> |  
 Christoph Lenting<sup>6</sup> | Yaohiro Inagaki<sup>7</sup> | Mike T. Harrison<sup>8</sup> | Jincheng Du<sup>9</sup>  |  
 Wenqing Xie<sup>9</sup> | Karine Ferrand<sup>10</sup> | Clare L. Thorpe<sup>11</sup> | Ramya Ravikumar<sup>11</sup> |  
 Claire L. Corkhill<sup>12</sup> | John S. McCloy<sup>1,13</sup>  | Michelle M. V. Snyder<sup>1</sup> |  
 Amanda R. Lawter<sup>1</sup> | Gary L. Smith<sup>1</sup> | R. Matthew Asmussen<sup>1</sup> | Joseph V. Ryan<sup>1</sup>

<sup>1</sup>Pacific Northwest National Laboratory, Richland, Washington, USA

<sup>2</sup>CEA, DES, ISEC, DPME, SEME, University of Montpellier, Montpellier, France

<sup>3</sup>Science & Technology Division, Corning Incorporated, Corning, New York, USA

<sup>4</sup>Actinide Chemistry Repository Science Program, Los Alamos National Laboratory – Carlsbad Operations, Carlsbad, New Mexico, USA

<sup>5</sup>Japan Atomic Energy Agency (JAEA), Ibaraki, Japan

<sup>6</sup>Institut für Geologie und Mineralogie, Universität zu Köln, Cologne, Germany

<sup>7</sup>Kyushu University, Fukuoka, Kyushu, Japan

<sup>8</sup>Waste Management and Decommissioning, National Nuclear Laboratory, Seascale, Cumbria, UK

<sup>9</sup>University of North Texas, Denton, Texas, USA

<sup>10</sup>Institute for Sustainable Waste & Decommissioning, Belgian Nuclear Research Centre (SCK CEN), Mol, Belgium

<sup>11</sup>University of Sheffield, Sheffield, UK

<sup>12</sup>School of Earth Sciences, University of Bristol, Bristol, UK

<sup>13</sup>Institute of Materials Research, Washington State University, Pullman, Washington, USA

**Correspondence**

Joelle T. Reiser, Pacific Northwest National Laboratory, Richland, WA, USA.  
 Email: [joelle.t.reiser@pnnl.gov](mailto:joelle.t.reiser@pnnl.gov)

**Present address**

Jonathan P. Icenhower, Actinide Chemistry Repository Science Program, Los Alamos National Laboratory –

**Abstract**

A new technique, termed the stirred-reactor coupon analysis (SRCA) method, has been developed to measure the rate of glass dissolution in forward-rate conditions. Monolithic glass coupons are partially masked with an inert material before placement in a large volume of well-mixed solution with known chemistry and temperature for a predetermined duration. After the test, the mask is removed, and the difference in step height between the protected area and the

This is an open access article under the terms of the [Creative Commons Attribution-NonCommercial-NoDerivs](https://creativecommons.org/licenses/by-nc-nd/4.0/) License, which permits use and distribution in any medium, provided the original work is properly cited, the use is non-commercial and no modifications or adaptations are made.

© 2025 Crown copyright. Corning Incorporated. Battelle Memorial Institute and The Author(s). International Journal of Applied Glass Science published by American Ceramics Society and Wiley Periodicals LLC. This article is published with the permission of the Controller of HMSO and the King's Printer for Scotland. This article has been contributed to by U.S. Government employees and their work is in the public domain in the USA.

Carlsbad Operations, Carlsbad, New Mexico, USA

### Funding information

Office of Environmental Management

exposed corroded portions of the sample coupon is measured to determine the extent of glass dissolution. The step height is converted to a rate measurement using the test duration and glass density. Test parameters such as sample surface preparation and test duration were evaluated to determine their effects on the measured rates. Additionally, results from an interlaboratory study (ILS) consisting of 12 laboratories from 11 different institutions are presented, where each laboratory performed 12 independent tests. When removing experimental outlier data, the 95% reproducibility limits for the SRCA method has no statistical difference with previously published standardized test methods used to determine the forward rate of glass dissolution. Overall, this paper describes steps necessary to perform the test method and provides the statistical calculations to evaluate test accuracy.

### KEYWORDS

chemical durability, dissolution, forward rate, test method

## 1 | INTRODUCTION

Glass corrodes upon contact with water, and elements from the glass are released into the contacting solution. This reaction is especially important in the field of nuclear waste management, as glass is used to immobilize radioactive material, and corrosion of the glass matrix would result in release of radionuclides into the near-field environment.<sup>1–3</sup> The fastest rate that the glass will corrode, known as the forward rate, is when the concentration of dissolved solids in the contacting solution is near zero and the system is in forward-rate conditions. Forward-rate measurements quantify the maximum dissolution rate of the glass at a given pH and temperature,<sup>4–10</sup> though it should be noted that the presence of certain ions in solution can also affect the forward rate.<sup>11</sup> Furthermore, if desired by the agency in charge of glass disposal, the forward rate can be used to set an upper bound for radionuclide release from glass in a disposal facility and can also be used to parameterize a portion of a glass dissolution rate equation. Assessments of forward dissolution rate are also relevant for commercial glasses, where even the relatively short-term exposure of glasses to aqueous media (e.g., cleaning/washing sheet glass, storing aqueous solutions in glass bottles, etc.) during product manufacturing or over product lifetime can engender observable glass dissolution effects and ultimately impact performance. Convenient methods to quantitatively assess forward-rate dissolution performance of different glass compositions can offer pragmatic benefits to the commercial glass industry, for example, rapidly screening candidate compositions across a range of possible exposure chemistries.

Measurements of forward rates have typically been performed with four different methods<sup>12</sup>: the single-pass flow-through (SPFT) method, the microchannel flow-through (MCFT) method, the Soxhlet test, and static dissolution tests. Each method employs a slightly different technique to measure the forward rate:

- The SPFT system is designed to enable a continuous flow of fresh solution into a reactor containing crushed glass without solution recirculation in the reactor. Collection of the effluent from the reactor allows monitoring of the release of elements from the glass as a function of time. To measure the forward rate, a series of flow-rate-to-surface-area ( $q/S$ ) tests are performed to find the  $q/S$  region where the glass dissolution rate stops increasing with further increases of  $q/S$  (i.e., far-from-equilibrium, or “dilute,” conditions).<sup>4,6,8,9,13–19</sup> The SPFT method is a consensus standard.<sup>20</sup>
- The MCFT test operates in a similar way as the SPFT, as fresh solution is passed over a glass surface; however, instead of placing a bed of crushed glass powder at the bottom of a reactor, a polished coupon is placed in a chamber where only a very small surface of glass is exposed to the solution that is assumed to flow parallel to the glass surface. In this manner, the glass dissolution rate can be measured both by analysis of the effluent solution and by measuring the extent of surface retreat of the glass coupon.<sup>21,22</sup>
- The Soxhlet apparatus was designed for dynamic leaching to measure the dissolution rate of glass at near neutral conditions in waters at a temperature between 50°C and 250°C.<sup>23</sup> The tests comprise a “Soxhlet compartment” containing a glass monolith, a round-bottom

flask, and reflux apparatus. The water is heated in the round-bottom flask until it evaporates, condenses at the top of the apparatus, drops on the glass monolith, and cycles back to the round-bottom flask. Periodic sampling of the water in the round-bottom flask allows for a measurement of the glass dissolution rate.

- In static dissolution tests, the release of elements from the glass is monitored by periodically removing solution samples from a reactor.<sup>24,25</sup> The duration of these tests is generally less than 8 h, and tests are performed at a low glass surface-area-to-solution-volume ( $S/V$ ) ratio. A forward rate is determined by discerning the time over which the release of elements is linear and congruent and assigning this regime as the forward rate. Solution feedback effects during the test duration are assumed to be negligible. The tests can be performed with a glass coupon or glass powder of known surface area.

Utilizing any of the four methods has certain benefits and shortcomings. In all tests, solution analysis is used to determine the release rate of all the elements, which can provide insight into the mechanisms of glass corrosion. The SPFT and MCFT are especially useful in locating test conditions where the glass is dissolving in forward-rate conditions. However, use of these methods is limited as solutions need to be analyzed, and multiple tests on each glass must be performed to isolate the test conditions that result in forward-rate conditions. For the SPFT test, where mixing through convective processes is assumed, complete mixing may not be achieved due to concentration gradients and preferential flow pathways in the reactor. This may result in solution gradients and a poor understanding of the solution chemistry in contact with the glass. Similarly, for the MCFT method, there has been evidence that the corrosion rate of the glass changes as the solution passes from the inlet to the outlet (i.e., a concentration gradient is established so that as the glass dissolves, the solution becomes more concentrated as it exits the reactor).<sup>21</sup> The greatest limitation for the Soxhlet test is that the pH of the solution in contact with the glass, which is established by the water condensing on the glass and the corrosion of the glass, is poorly understood. Lastly, in the static dissolution tests, as the glass dissolves, the system quickly moves from far-from-equilibrium conditions towards equilibrium, making it difficult to determine how long forward-rate conditions were maintained. Additionally, if mixing in the reactor is not adequate, this would result in changes in pH near the glass surface that may not be the same as the bulk solution pH, which can preclude isolating the impact of bulk pH on the forward dissolution rate.

The stirred-reactor coupon analysis (SRCA) method was developed as an alternative to overcome some of the lim-

itations of the other tests, such as the need for extensive solutions analysis and possible mixing issues. The evolution of the SRCA method was inspired by studies utilizing vertical scanning interferometry (VSI), a solid-state characterization technique that can be used to observe phase separation on glass coupons where the different phases dissolve at different rates.<sup>16,26</sup> The VSI method has also been used to examine the weathering of crystalline silicate minerals<sup>27–29</sup> and the relative corrosion rate of multiphase materials such as cements and glass-ceramics.<sup>30–32</sup> In glass corrosion tests by Icenhower et al.,<sup>26</sup> a portion of a glass coupon was covered with an inert glue to preserve a portion of unreacted glass surface. The glass coupons were then placed in a SPFT setup and allowed to corrode for a given duration. Icenhower and Steefel<sup>16</sup> determined that the dissolution rate measured from the surface retreat of the monolithic sample with VSI was within uncertainty of the dissolution rates determined from the analysis of solutions. The evidence that monolithic and solution dissolution rates agreed, coupled with the indication that the surface retreat could be used to index the relative dissolution rate of multiphase materials, led to a further evolution of the experiment. Specifically, Crum et al.<sup>33</sup> used the method developed by Icenhower et al.<sup>26</sup> to examine the dissolution of ten  $1 \times 1 \times 0.1$  cm glass-ceramic monoliths placed in the same 500-mL reactor. To maintain low solution activities of elemental species released from the glass-ceramics, the solution flow rate to glass surface area ratio was increased to limit solution feedback effects.

After the set of experiments by Crum et al.,<sup>33</sup> it was theorized that forward-rate conditions could be maintained if the flow rate from a given test duration was converted to a total volume. If the same glass surface area was maintained, then a  $q/S$  in a test where the glass dissolved at a forward rate could be converted to a volume-to-surface area ( $V/S$ ) ratio where solution feedback effects should be negligible. Thus, a final system design was developed where one or several masked glass coupons were placed in a large container with a large solution volume. To ensure that the solution was well-mixed, the reactor was stirred, and the resulting system was named the SRCA. In SRCA, the glass is reacted for a predetermined period of time in a solution with controlled pH and temperature, and the measured glass dissolution rate is determined to be the forward rate.

The SRCA method is similar to the Icenhower and Steefel<sup>16</sup> method in that it involves masking monolithic glass coupons with an inert material; however, rather than placing the coupons in an SPFT system, the coupons are placed in a large volume of well-mixed solution with known chemistry and temperature for a predetermined duration. After terminating the test, the mask is

removed and the step height difference between the protected area under the mask and the exposed corroded portions of the sample coupon is measured to determine the extent of glass dissolution. The step height is converted to a rate measurement using the test duration and glass density. The method has recently been accepted as ASTM International test method C1926-23 “Standard Test Method for Measurement of Glass Dissolution Rate Using Stirred Dilute Reactor Conditions on Monolithic Samples.”<sup>34</sup> The present paper describes development and application of the SRCA method. This includes a description of the design of the system, the effect of certain experimental variables (i.e., coupon polish and test duration), and an assessing the precision (repeatability) and reproducibility of the SRCA technique. To measure test reproducibility, an interlaboratory study (ILS) involving 12 independent laboratories from 11 different institutions was performed. Each institution evaluated 12 test conditions (four glass compositions in three pH–temperature combinations). A description of the technique, common experimental control issues, and the statistics associated with the ILS are provided, specifically the method precision and bias.

## 2 | MATERIALS AND METHODS

### 2.1 | SRCA test reactor design

The forward rate of glass dissolution is measured by placing a glass sample in a relatively large volume of dilute aqueous solution. This is the basis behind the SRCA test and the subsequent reactor design (Figure 1). The SRCA test reactor used in the ILS was a 9.5 L 316 stainless-steel reactor (2.5 US Gallon, McMaster Carr, part number 41815T2) with an eight-sample capacity. The inner dimension of the reactor is 23.8 cm diameter and 23.8 cm in height. The lid has a diameter of 27.0 cm and there are two opposed handles with a total width in that direction of 30.5 cm. Active agitation and a four-bladed baffle system was developed to ensure well-mixed conditions (i.e., turbulent flow conditions) in the reactor chamber to minimize concentration gradients near the dissolving glass. The four stainless-steel baffles are equally spaced, 1.90 cm wide, 0.318 cm thick, 20.3 cm in length, and spaced 0.635 cm off the wall. Figure 1 gives a photograph of the 8-port reactor. General mixing guidelines were used to design reactors with appropriate mixing near the sample surfaces<sup>35</sup> and are applied as detailed in the annex of the SRCA ASTM standard.<sup>36</sup> Additional tests at the Pacific Northwest National Laboratory (PNNL) were performed in larger versions of the ILS reactors (~20 L) with 15 sample capacity. These results were included in the ILS calcula-



**FIGURE 1** A photograph of the 8-port stirred-reactor coupon analysis (SRCA) reactor used in the interlaboratory study (ILS). The image shows the lid, propeller, baffles, and a glass coupon in the foreground. This combination of pieces is placed in the stainless-steel reactor shown in the background. The inner dimension of the reactor is 23.8 cm diameter and 23.8 cm in height.

tions. Additional design details for the 8-sample reactors are provided in Supporting Information Section 1.

After filling the reactor to 19.8 cm height, the solution is mixed at 60 rpm with a stainless-steel propeller (316 stainless steel, McMaster Carr, part number 8004K3, 12.7 cm diameter, 3.18 cm height with a stir shaft length of 0.95 cm and total length of 30.5 cm). The propeller is inserted in the pot through a center hole in the lid.

Each glass coupon is held in place by a stainless-steel alligator clip attached to a stainless-steel rod (0.318 cm diameter and 15.2 cm long), which was itself held in place with a high-temperature rubber seal. There are eight holes through which glass monoliths are placed in the reactor. Each sample hole is 1.27 cm in diameter and 7.62 cm off center. The sampling port was fitted with a similar seal, and the impeller shaft feed-through is fitted with a Teflon ferrule. Together, these seals minimize solution evaporation while maintaining easy access to samples and solution. There is one sample port (1.90 cm diameter and 6.35 cm off center), which is available to remove an aliquot of the leachant if desired. Each participating group was sent an SRCA testing system package from PNNL that included all items necessary to perform SRCA tests.

### 2.2 | Experimental method for the SRCA test

The method for SRCA is described in complete detail in ASTM C192623. A summary of the conditions used for this study is provided here.



**FIGURE 2** Examples of masked coupons before stirred-reactor coupon analysis (SRCA) testing. The ruler scale is in centimeters with millimeter demarcations.

### 2.2.1 | Glass monolith preparation

Glass monoliths were cut from larger glass specimens with dimensions of approximately 10 mm × 15 mm × 2 mm. One face of each monolith was polished in sequential finishes with various size polishing media (i.e., 15 μm, 9 μm, etc.) to a final finish of 3 μm. Some additional coupons were further polished to 1 μm and 0.05 μm (colloidal silica) finishes for a small study on the effects of polishing on the dissolution rate. The polished coupons were cleaned with acetone and ethanol and then air-dried. A silicone mask (Permatex® Clear Room Temperature Vulcanizing silicone) was applied on approximately ¼ of the surface area of the polished face and allowed to cure overnight. Figure 2 shows examples of masked coupons prepared for SRCA testing.

### 2.2.2 | Solution preparation

Solutions with target pH values at room temperature ( $pH_{RT}$ ) of 10 and 11 were used for SRCA tests in this study. These conditions were chosen as these pH-temperature combinations result in a step height of more than 1000 nm for a typical glass in the desired test duration. The  $pH_{RT}$  10 solutions were buffered with 0.05 M tris(hydroxymethyl)aminomethane (TRIS) in ASTM Type I water deionized water (DIW),<sup>37</sup> and adjusted to the target  $pH_{RT}$  with 15.8 M HNO<sub>3</sub> and/or 1 M LiOH solutions to  $pH_{RT}$  10.0–10.3. The  $pH_{RT}$  11 solutions were prepared using 0.019 M LiCl and 0.001 M LiOH in DIW and were adjusted to  $pH_{RT}$  11.0–11.3 with 15.8 M HNO<sub>3</sub> and/or 1 M LiOH solutions. Each SRCA experiment required 8.8 L of solution for the 8-port reactors and 16.5 L for the 15-port reactors.

### 2.2.3 | Test procedure

Before use, new reactors and parts were washed with detergent (e.g., generic dish soap or an industrial cleaner such as Micro-90®) to degrease all machine parts, followed by successive rinses with ethanol, DIW, ~0.15 M HNO<sub>3</sub>, and DIW. Then, the reactor was fully assembled, filled with DIW, and held at 90°C ± 10°C overnight. The pH of the solution was then measured and if the pH was between 5.0 and 7.0, the reactor was ready for use.

To initiate a test, the target volume of prepared solutions was added into test reactors and heated to test temperature (i.e., 40°C or 70°C) in an oven overnight. These temperatures were selected as these values are in the range of test temperatures typically used for nuclear waste glass durability testing. After the solution was heated, the coupons were inserted into the reactor through a marked port on the reactor lid, and the time that the glass was placed in the reactor was recorded. The temperature was monitored daily, and  $pH_{RT}$  of solution aliquots were monitored frequently: at the beginning and end of the experiments (for experiments with durations less than 1 week, or at least twice a week for experiments lasting longer than 1 week. Any pH drift detected during an experiment was corrected with small additions of HNO<sub>3</sub> and/or LiOH solutions. The pH drift was likely due to CO<sub>2</sub> solubility in the pH-controlled solution that causes the pH to become more acidic. Weekly evaporation checks were performed to ensure that no more than 10% of the solution evaporated through visual observations of the solution height in the reactor. Evaporated solution amounts were renewed with DIW as needed. The addition of DIW was relatively small and the change in pH of the solution was within measurement uncertainty (0.1 pH units) after the DIW additions were performed. Thus, the experimental conditions could be considered constant throughout the duration of the experiment.

After the specified test duration, the monoliths were removed from the reactor, rinsed three times with DIW and three times with ethanol, and then air-dried. The end-of-test solution pH and dried monolith mass are recorded. The silicone masks were removed from the altered monoliths with razorblades and ethanol-soaked cotton swabs. Various techniques were used to quantify the step height between the altered and masked (i.e., presumed unaltered) surfaces including optical profilometry, stylus profilometry, scanning electron microscopy, confocal microscopy, and atomic force microscopy. A target step height was typically 1000–5000 nm. This range was selected based on ease of measurement but heights outside of this range are possible. Locating the duration required to reach this step height range for a glass composition in a given set of test conditions requires either knowledge of the glass dissolution rate or pretesting of the glass.

## 2.3 | Calculation of dissolution rate

Based on the difference in height measured between the dissolved (exposed) and reference (masked) surfaces on the glass monolith, a dissolution rate ( $\text{g m}^{-2} \text{d}^{-1}$ ) was determined using the step height ( $h$  in m), the experimental duration ( $t$  in d), and glass density ( $\rho$  in  $\text{g m}^{-3}$ ) via Equation (1):

$$\text{rate} = \frac{h \times \rho}{t} \quad (1)$$

## 2.4 | Interlaboratory study description

This section introduces the participants involved in the ILS, the selected glasses, and the test conditions used in the ILS. ASTM E691-23<sup>38</sup> was followed for experimental design and analysis of data of the ILS.

### 2.4.1 | Participants

Participating laboratories familiar with glass corrosion testing were identified for the ILS SRCA experiments and included two independent laboratory groups at PNNL and 10 additional laboratories from seven countries. The study was led and coordinated by PNNL. The data collected from the institutions are presented in anonymous fashion in the results section, with each of the twelve collaborating groups assigned a random letter designation from A to L. The number of participating labs is in compliance with the ASTM procedure to conduct an ILS of precision (i.e., minimum eight participating laboratories at the start of study, with results reported from a minimum of six laboratories).<sup>38</sup>

### 2.4.2 | Glass compositions

Four glass compositions were selected to represent simulant nuclear waste glass composition variances and to provide a range of dissolution rates that would be measurable for the proposed test parameters (Table 1). To ensure a blind test for the ILS, the glasses were designated A, B, C, and D upon shipment to the participants from PNNL. Only PNNL staff managing the ILS (one of the two PNNL locations) were aware of the glass identities before testing.

The LAWA44 glass composition (Glass A) was selected for testing because it is a baseline glass for Hanford low-activity waste (LAW) vitrification<sup>39,44</sup> that has been the subject of extensive testing. Forward rates have been previously established for this composition using the SPFT test method.<sup>6</sup> Glass B was the low-activity reference mate-

rial (LRM)<sup>40</sup> and was chosen for SRCA testing because the LRM glass was previously used for the SPFT ILS.<sup>20</sup> The International Simple Glass-2 (ISG-2) was selected as Glass C because of its use within the international nuclear waste glass waste forms community.<sup>41</sup> Finally, a composition from the 2019 Low-Activity Waste Glass Standards (LGS19) series that were fabricated as composition analysis standards for the Hanford Waste Treatment and Immobilization Plant (WTP) was selected.<sup>45</sup> Of the seven LGS19 compositions, the LGS19-03 composition was selected for Glass D as it had the highest predicted Product Consistency Test Method A (PCT-A) response,<sup>46</sup> a common method to assess glass durability, and thus made a good candidate for this study. An additional two glasses (eLAW21 and eLAW23<sup>42</sup>) were selected for an initial study at PNNL to determine the effect of test duration on the measured dissolution rate.

### 2.4.3 | Test conditions

The SRCA ILS tests were performed for all four glasses at a series of defined starting pH values and temperatures (Table 2). The  $\text{pH}_{\text{RT}} 11.0/70^\circ\text{C}$  condition (used for Tests 1 and 4) was used in the SPFT ILS which included LRM (i.e., Glass B), which allows for a direct comparison of the results between the SRCA ILS and the SPFT ILS. Participants were instructed to place any eight of the glass coupons concurrently in the reactor. Glass samples were polished at PNNL or at the participant laboratory. Each experiment was run for at least the minimum duration described in Table 2. Directions specified that the large, polished coupon face should be oriented towards the impeller.

For Test 4, two coupons of Glass B and Glass D were included in the reactor. The remaining testing slots were optionally filled with other materials provided by each participating laboratory to test, such as other glasses, glass-ceramics, or cementitious waste forms. Alternatively, one or all of the remaining slots could remain empty, at the discretion of the participating laboratory. Test 4 was designed to ensure consistent results even when other unrelated samples with various corrosion behaviors are tested in the same reactor. Results for the materials that were not Glass A–D are not discussed in the present manuscript.

## 3 | RESULTS AND DISCUSSION

### 3.1 | Effect of experimental conditions

Prior to the ILS test, the effects of polishing and test duration were examined at PNNL to assess their impact on test results. A Bruker optical profilometer was used to measure

**TABLE 1** As-measured glass compositions in mass % for glasses used in interlaboratory study (ILS) testing: LAWA44,<sup>39</sup> low-activity reference material (LRM),<sup>40</sup> International Simple Glass-2 (ISG-2),<sup>41</sup> and LGS1903.<sup>42</sup>

	LAWA44 "Glass A"	LRM "Glass B"	ISG-2 "Glass C"	LGS19-03 "Glass D"	eLAW21	eLAW23
Al <sub>2</sub> O <sub>3</sub>	6.01	9.51	5.96	6.92	6.51	8.30
B <sub>2</sub> O <sub>3</sub>	9.17	7.85	17.38	13.24	9.35	12.50
CaO	2.06	0.54	2.51	2.02	4.30	1.25
CdO	—	0.16	—	—	—	—
Cl	0.47	—	0.04	0.18	0.50	0.52
Cr <sub>2</sub> O <sub>3</sub>	0.02	0.19	—	0.49	0.25	0.26
F	0.01	0.86	—	0.4	1.40	1.47
Fe <sub>2</sub> O <sub>3</sub>	7.10	1.38	0.01	1.41	0.32	0.33
HfO <sub>2</sub>	—	—	0.05	—	—	—
K <sub>2</sub> O	0.50	1.5	0.01	4.75	0.90	0.94
La <sub>2</sub> O <sub>3</sub>	—	0.02	0.12	—	—	—
Li <sub>2</sub> O	—	0.11	—	0.808	—	—
MgO	1.98	0.1	1.76	0.49	1.36	1.42
MnO <sub>2</sub>	—	0.08	0.01	—	—	—
MoO <sub>3</sub>	0.09	0.1	—	—	—	—
Na <sub>2</sub> O	20.91	20.03	12.10	16.22	21.69	27.11
NiO	—	0.19	—	—	—	—
P <sub>2</sub> O <sub>5</sub>	0.03	0.54	0.01	0.52	0.40	0.42
Re <sub>2</sub> O <sub>7</sub>	0.07	—	—	—	—	—
SiO <sub>2</sub>	44.07	54.20	56.87	37.48	45.90	39.90
SnO <sub>2</sub>	—	—	0.06	0.93	1.43	0.75
SO <sub>3</sub>	0.12	0.30	0.01	0.6	0.53	0.55
TiO <sub>2</sub>	1.98	0.10	0.01	0.5	—	—
V <sub>2</sub> O <sub>5</sub>	—	—	—	2.27	0.46	0.49
Y <sub>2</sub> O <sub>3</sub>	—	—	—	0.76	—	—
ZnO	3.07	—	—	3.57	2.90	3.04
ZrO <sub>2</sub>	2.99	0.93	3.31	5.72	1.81	0.77
Totals	100.65	98.69	100.22	99.28	100.00	100.00
Density (g cm <sup>-3</sup> )	2.694 <sup>43</sup>	2.557 <sup>43</sup>	2.475 <sup>43</sup>	2.710 <sup>43</sup>	2.69 <sup>42</sup>	2.69 <sup>42</sup>

Also included are two target compositions of glasses used at Pacific Northwest National Laboratory (PNNL) to assess the impact of test duration on the measured dissolution rate (eLAW21 and eLAW23).

**TABLE 2** Test conditions for each test number.

Test number	pH	Temperature	Minimum duration
1	11	70°C	1 day
2	10	70°C	7 days
3	11	40°C	9 days
4	11	70°C	1 day

the step height between the altered and unaltered surfaces for all coupons at PNNL which has measurement uncertainties on the nanometer scale. In addition, the influence of other materials in the test reactor was tested during the ILS.

### 3.1.1 | Effect of polish

Glass B was used to determine the effect of polishing on measured dissolution rates at pH<sub>RT</sub> 11.0/70°C. Glass B monoliths were polished to three different finishes: three to 3 μm, three to 1 μm, and four to 0.05 μm (colloidal silica). All monoliths were tested for 5 days. This investigation was performed because surface roughness increases the apparent surface area available to react with the bulk solution and the techniques used to assess the step height may be sensitive to the surface roughness. Figure 3 shows that the measured dissolution rate was relatively consistent across replicate coupons and regardless of the finish for the range of finishes evaluated here. The average

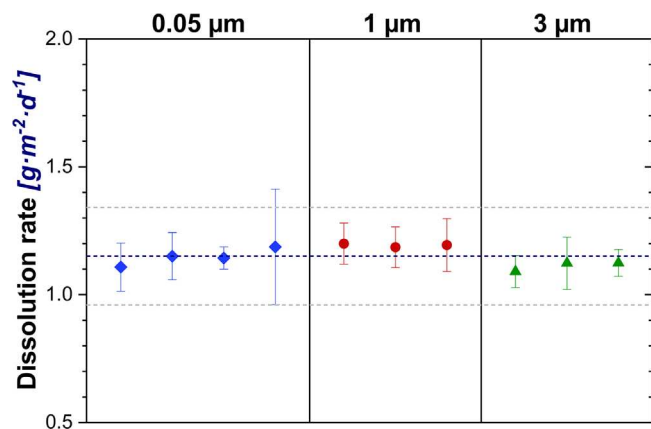


**FIGURE 3** Average dissolution rates of Glass B at  $\text{pH}_{\text{RT}} 11.0/70^\circ\text{C}$  polished to 0.05, 1, and 3  $\mu\text{m}$ . Uncertainties are represented by one standard deviation from three rate measurements per coupon, with each panel showing results from several replicate coupons per polish level. The center dashed line represents the overall average of all measurements on the Glass B coupons tested for evaluating polishing effects, and the outer dashed lines represent two standard deviations (30 measurements total).

dissolution rates and standard deviations (calculated from three measurements per coupon) were  $1.15 \pm 0.12 \text{ g m}^{-2} \text{ d}^{-1}$ ,  $1.19 \pm 0.08$ , and  $1.11 \pm 0.07$  for 0.05  $\mu\text{m}$ , 1  $\mu\text{m}$ , and 3  $\mu\text{m}$  polish levels, respectively. The average dissolution rate and standard deviation for all samples regardless of polishing were  $1.15 \pm 0.10 \text{ g m}^{-2} \text{ d}^{-1}$ . The results indicate 3  $\mu\text{m}$  polish gives functionally equivalent data to those polished to submicrometer levels with colloidal silica; therefore, additional polishing beyond a 3  $\mu\text{m}$  finish is not needed.

### 3.1.2 | Effect of duration

The glasses eLAW21 and eLAW23 were studied to measure the effect of duration on the glass dissolution rates at  $\text{pH}_{\text{RT}} 11.0/70^\circ\text{C}$  to determine if the experimental run time would affect the measured dissolution rate (i.e., if the measured dissolution rate changes as the reaction progresses). All glasses were tested in the same reactor. The eLAW21 and eLAW23 monoliths were removed at 0.5, 1, 3, and 6 days (except an eLAW21 sample was not removed at 0.5 days due to the limited number of available coupons). Figure 4 shows measured dissolution rates from samples removed at the different durations. Coupons were removed from the reactor at the specified duration and the average dissolution rates and standard deviations (calculated using three measurements on each coupon) for all durations were  $2.48 \pm 0.12 \text{ g m}^{-2} \text{ d}^{-1}$  and  $7.97 \pm 0.45 \text{ g m}^{-2} \text{ d}^{-1}$  for eLAW21 and eLAW23, respectively. For these glasses and conditions, the dissolution rates were within uncertainty regardless of duration; therefore, the dissolution rates did not change for the first 6 days

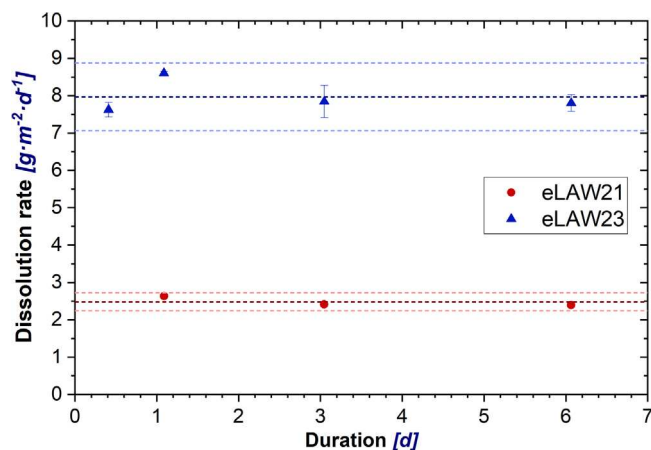


**FIGURE 4** Average dissolution rates for coupons of eLAW21 and eLAW23 altered in the same stirred-reactor coupon analysis (SRCA) reactor for different durations. Uncertainties are represented by one standard deviation. The center dashed lines through the respective data set represent the overall average of all coupons tested and the outer dashed lines represent two standard deviations.

of testing. It is unknown if there would be further changes to dissolution rates if the reaction were allowed to go longer.

### 3.1.3 | Influence of other materials in reactor

The ILS included Test 4, which had the same experimental conditions as Test 1 ( $\text{pH}_{\text{RT}} 11/70^\circ\text{C}$ , 1 day), to evaluate the influence of having other materials present in the reaction reactor (or the other sample positions empty) on the dissolution rates of Glasses B and D. As a reminder, Test 1 vessels contained only Glasses A–D while Test 4 contained Glasses B and D and various other glasses chosen by each laboratory without informing the other laboratories. Figure 5 shows the average dissolution rates and standard deviations of Glasses B and D determined from data collected by all participants for Tests 1 and 4. The averages and standard deviations are similar regardless of the test condition. The results indicate that the presence of other materials in the test reactor had no discernable effect on the average dissolution rate of Glasses B and D, implying the presence of other samples does not significantly affect the test responses.

## 3.2 | Experimental control issues

As a result of the ILS testing, there were two areas that were noted where experimental control was difficult: pH stability and alteration layer formation. The pH was difficult to maintain, particularly at  $\text{pH}_{\text{RT}} 11$  where there was

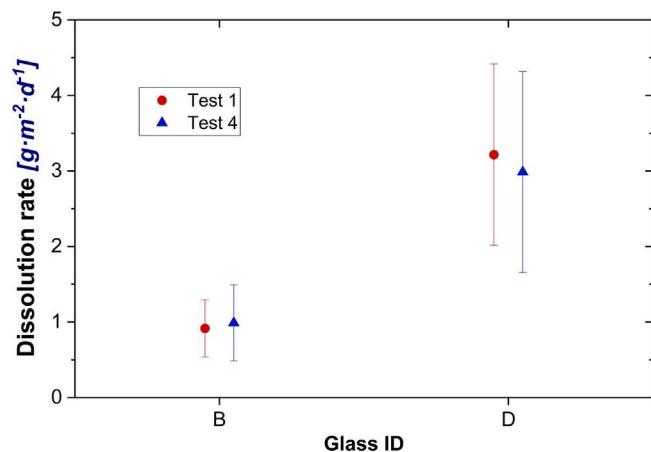


FIGURE 5 Average dissolution rates for glasses B and D in  $\text{pH}_{\text{RT}} 11/70^\circ\text{C}$  conditions for Test 1 and Test 4. Uncertainties are represented by one standard deviation.

a common decrease in pH observed by all the laboratories. This decrease is attributed to  $\text{CO}_2$  uptake from the atmosphere into solution as  $\text{H}_2\text{CO}_3$ . To correct for this, the pH was adjusted by either adding LiOH solution to raise the pH or allowing the solution pH to stabilize for 13 days before starting the test. Even with the actions made to control pH, measured  $\text{pH}_{\text{RT}}$  ranged from 10.31 to 11.18 for the  $\text{pH}_{\text{RT}} 11/70^\circ\text{C}$  condition, from 9.71 to 10.01 for the  $\text{pH}_{\text{RT}} 10/70^\circ\text{C}$  condition, and from 9.20 to 11.04 for the  $\text{pH}_{\text{RT}} 11/40^\circ\text{C}$  condition. Various approaches were considered to account for the difficulty in accounting for the pH effect on the rate measurement and are described in the precision and bias section (Section 3.3).

In addition to difficulties in controlling the solution pH, alteration layers were observed on the surfaces of some glass samples, especially Glass A and Glass D at  $\text{pH}_{\text{RT}} 11$ . The alteration layer was identified either by iridescence after the monolith was removed from solution or by the presence of steps of intermediate height observed on the altered surface. In all cases, the maximum height difference between the altered and unaltered surfaces was used for the analysis, providing the fastest dissolution rate, which would be the most conservative approach if the maximum glass dissolution rate was used as an upper bound for radionuclide release from glass in a disposal facility. Reasons for the formation of the alteration layer are presently beyond the scope of this study and the use of data from glasses that form an alteration layer is at the discretion of the user (although discussed in ref.<sup>16</sup>).

### 3.3 | Method precision and bias

The dissolution rates for each glass composition from each laboratory at each  $\text{pH}_{\text{RT}}$ /temperature combination

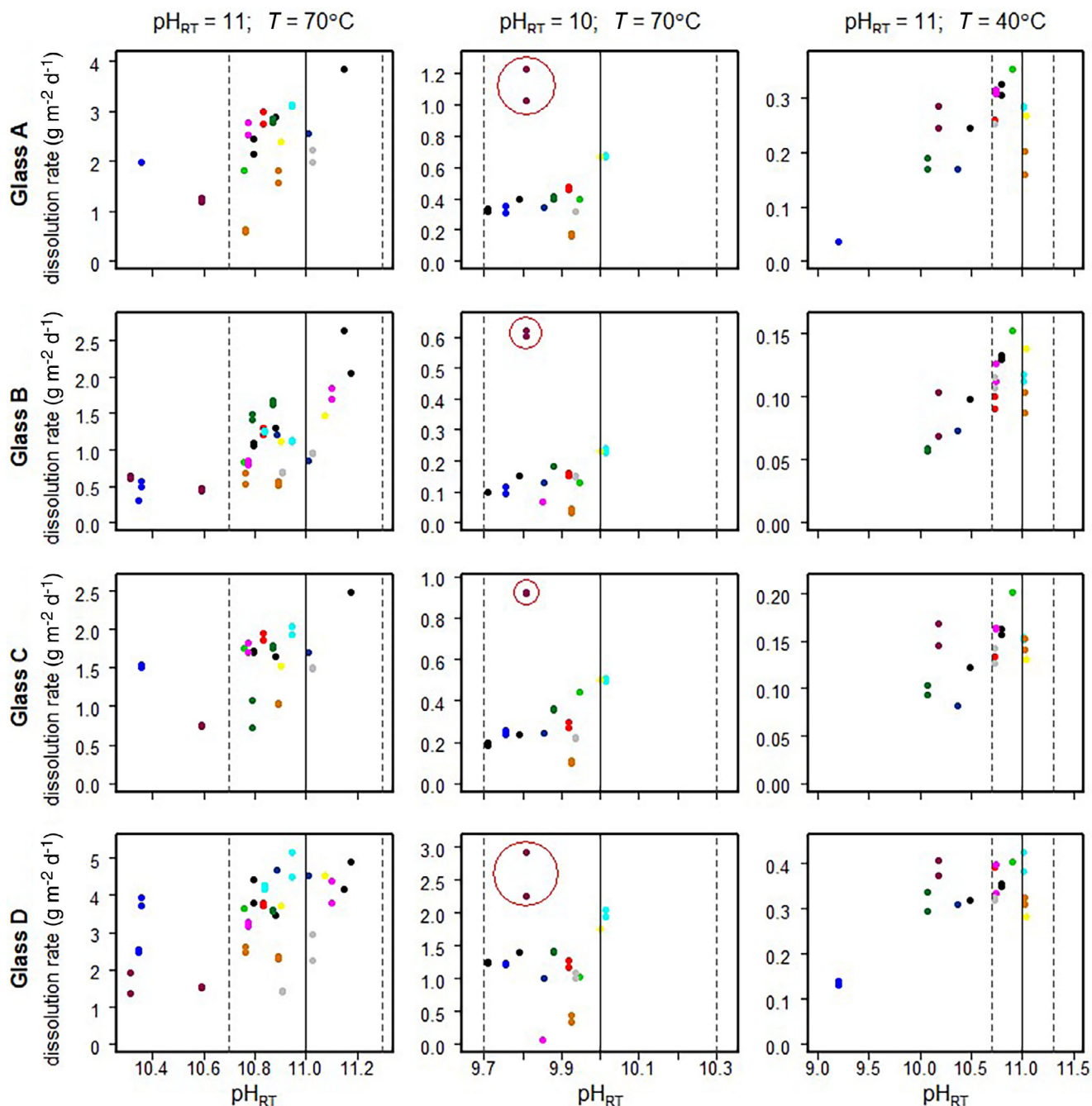
for the four glasses are presented in Figure 6, where the  $\text{pH}_{\text{RT}}$  is the average  $\text{pH}_{\text{RT}}$  calculated from the  $\text{pH}_{\text{RT}}$  values provided by each laboratory. In general, the dissolution rates are highest at  $\text{pH}_{\text{RT}} 11/70^\circ\text{C}$ , become lower at  $\text{pH}_{\text{RT}} 10/70^\circ\text{C}$ , and are lowest at  $\text{pH}_{\text{RT}} 11/40^\circ\text{C}$ . This pattern was observed for all glasses in the study. Similarly, the glass compositions showed a consistent pattern from highest to lowest observed dissolution rates regardless of condition: Glass D > Glass A > Glass C > Glass B. Additionally, the measured  $\text{pH}_{\text{RT}}$  values tended to drift towards neutral for all glass/condition combinations used in this study due to the  $\text{CO}_2$  uptake in the reactor as the experiment progressed.

Figure 6 also shows that certain dissolution rates for the individual test conditions were outliers either due to a large deviation from the target  $\text{pH}_{\text{RT}}$  (>0.3  $\text{pH}_{\text{RT}}$  units from target) or because of experimental inconsistencies resulting in a particular laboratory (L) reporting higher dissolution rates than those disclosed by other laboratories for tests conducted at  $\text{pH}_{\text{RT}} 10/70^\circ\text{C}$ . Various determinations of method precision and bias were performed to account for these outliers. Additionally, a pH-corrected dissolution rate approach was pursued to address the difficulty in controlling the  $\text{pH}_{\text{RT}}$ . In total, five different cases were performed to evaluate the method precision and bias:

- Case 1: All data were included.
- Case 2: Experimental outliers (i.e., dissolution rates from institution L at  $\text{pH}_{\text{RT}} 10/70^\circ\text{C}$ ) were excluded.
- Case 3: Experimental outliers (i.e., dissolution rates from institution L at  $\text{pH}_{\text{RT}} 10/70^\circ\text{C}$ ) and dissolutions rates from tests where the  $\text{pH}_{\text{RT}}$  was not controlled to within 0.3 pH units of the target  $\text{pH}_{\text{RT}}$  were excluded.
- Case 4: All data are included, but dissolution rates have been corrected using a pH-rate linear equation.
- Case 5: Dissolution rates have been corrected using a pH-rate linear equation (like Case 4), but experimental outliers (i.e., dissolution rates from institution L at  $\text{pH}_{\text{RT}} 10/70^\circ\text{C}$ ) were excluded.

As Case 1 and Case 4 are very similar to Case 2 and Case 5, respectively, they are discussed in Supporting Information Section 2. Precision is defined as the closeness of agreement between independent test results obtained under stipulated conditions while the bias is the difference between the expectation of the test results and an accepted reference value.<sup>38</sup> Bias is the total systematic error whereas precision depends on random errors. Precision is generally computed as a standard deviation of test results.

For each case, a repeatability standard deviation ( $s_r$ ), reproducibility standard deviation ( $s_R$ ), repeatability limit ( $r$ ), and reproducibility limit ( $R$ ) were calculated for each glass and condition. These parameters are defined in



**FIGURE 6** Individual dissolution rates for each glass in all test conditions. Test 1 and 4 results are plotted together as the test conditions were the same. Colors represent results from laboratories A to L. The solid vertical lines represent target  $\text{pH}_{\text{RT}}$ , and the dashed lines represent 0.3 pH units away from target  $\text{pH}_{\text{RT}}$ . The  $\text{pH}_{\text{RT}}$  is the average  $\text{pH}_{\text{RT}}$  calculated from the  $\text{pH}_{\text{RT}}$  values provided by laboratories A–L for the different test conditions. The datapoints circled in red were excluded as experimental outliers in Cases 2, 3, and 5.

ASTM E691-23, and the equations used to calculate the parameters are described in ASTM E691-23 Appendix A2 as the data sets are unbalanced (some institutions did not test a duplicate sample). In general,  $s_r$  represents the variability associated with replicate samples tested by the same institution (intralaboratory), that is, duplicate pairs or instances where an experiment had two coupons of the same glass that produced detectable step heights in the

same reactor, whereas  $s_R$  represents the variability associated with replicate samples tested by multiple laboratory (interlaboratory) and are calculated from all available test results for a given glass and condition combination. The  $r$  and  $R$  parameters are simply  $2.8 \times s_r$  and  $2.8 \times s_R$  for the 95% repeatability and reproducibility limits, respectively. The design of the ILS resulted in nearly all the experiments to be performed in duplicate. Because the

**TABLE 3** Average dissolution rates and standard deviations at various pH (nominal and average measured reported with one standard deviation) and temperature (nominal only) values from the interlaboratory study (ILS) study for Case 2.

Glass ID	pH <sub>RT</sub>	T (°C)	N	Measured	Average Rate	s <sub>r</sub>	R	s <sub>R</sub>	R
				pH <sub>RT</sub>	(g m <sup>-2</sup> d <sup>-1</sup> ) <sup>a</sup>				
A	11	70	25	10.8 ± 0.2	2.25 ± 0.79	0.13	0.36	0.80	2.24
	10	70	18	9.9 ± 0.1	0.40 ± 0.15	0.01	0.04	0.15	0.42
	11	40	22	10.5 ± 0.5	0.24 ± 0.08	0.02	0.04	0.08	0.24
B	11	70	40	10.8 ± 0.2	1.04 ± 0.51	0.05	0.14	0.52	1.45
	10	70	19	9.9 ± 0.1	0.14 ± 0.06	0.01	0.02	0.06	0.17
	11	40	20	10.7 ± 0.3	0.10 ± 0.03	0.01	0.03	0.03	0.07
C	11	70	25	10.8 ± 0.2	1.55 ± 0.44	0.09	0.25	0.44	1.24
	10	70	18	9.9 ± 0.1	0.29 ± 0.13	0.01	0.03	0.13	0.36
	11	40	20	10.7 ± 0.3	0.14 ± 0.03	0.01	0.02	0.03	0.08
D	11	70	38	10.8 ± 0.2	3.32 ± 1.08	0.26	0.73	1.09	3.06
	10	70	20	9.88 ± 0.09	1.12 ± 0.54	0.05	0.14	0.56	1.56
	11	40	22	10.5 ± 0.5	0.33 ± 0.08	0.02	0.06	0.08	0.22

The  $N$ ,  $s_r$ ,  $r$ ,  $s_R$ , and  $R$  values for each condition are also provided.

<sup>a</sup>Uncertainty is presented as one standard deviation of all reported rate values considering the total number of tests performed ( $N$ ).

instances were duplicates rather than higher multiples, in this case a standard deviation cannot be used to determine repeatability. Instead, the relative distance of each data-point from the average of the pair was analyzed to achieve a determination of how consistent measurements of different coupons of the same glass in the same reactor can be expected.

### 3.3.1 | Case 2 (removal of dissolution rate outliers)

The calculations for the experimental outlier results for Case 1 are included in Supporting Information Table 2. Case 2 was examined to account for the outlier rates for all glasses for the pH<sub>RT</sub> 10/70°C condition (circled values in Figure 6) reported from institution (L). The outlier rates were due to experimental issues that arose during the testing, attributed to possible inadequate cleaning of the vessel reported by the institution that provided the outlier rates. Thus, for Case 2, test results obtained from all 12 laboratories are included for the pH<sub>RT</sub> 11/70°C and pH<sub>RT</sub> 11/40°C calculations, but 11 laboratories were included for pH<sub>RT</sub> 10/70°C where results from institution L data were excluded. A summary of Case 2 with the average dissolution rates reported with one standard deviation, average measured pH<sub>RT</sub> values with one standard deviation, and the number of test results ( $N$ ) for each glass and condition excluding the outlier values are reported in Table 3. Table 3 also provides the repeatability terms  $s_r$  and  $r$  determined from the duplicate test results from the same institution for each glass and condition for Case 2.

The  $s_r$  range from 3% of the average rate (i.e.,  $0.40 \pm 0.01$  g m<sup>-2</sup> d<sup>-1</sup> for glass A at pH<sub>RT</sub> 10/70°C) to 10% of the average rate (i.e.,  $0.10 \pm 0.01$  g m<sup>-2</sup> d<sup>-1</sup> for glass B at pH<sub>RT</sub> 11/40°C), indicating the repeatability of the method for the tested glasses and conditions is between 3% and 10% of the average rates for Case 2. The corresponding  $r$  values are therefore 10% of the average rate for glass A at pH<sub>RT</sub> 10/70°C (i.e.,  $0.40 \pm 0.04$  g m<sup>-2</sup> d<sup>-1</sup>) and 30% for glass B at pH<sub>RT</sub> 11/40°C (i.e.,  $0.10 \pm 0.03$  g m<sup>-2</sup> d<sup>-1</sup>).

The reproducibility terms  $s_R$  and  $R$  for test results from all institutions for each glass and condition for Case 2 are also provided in Table 3. The  $s_R$  range from 20% of the average rate (i.e.,  $0.14 \pm 0.03$  g m<sup>-2</sup> d<sup>-1</sup> for glass C at pH<sub>RT</sub> 11/40°C) to 50% of the average rate (i.e.,  $1.04 \pm 0.52$  g m<sup>-2</sup> d<sup>-1</sup> for glass B at pH<sub>RT</sub> 11/70°C), indicating the reproducibility of the method for tested glasses and conditions is between 20% and 50% for Case 2. The corresponding  $R$  values (i.e., the 95% reproducibility limit) are 60% of the average rate for glass C at pH<sub>RT</sub> 11/40°C (i.e.,  $0.14 \pm 0.08$  g m<sup>-2</sup> d<sup>-1</sup>) and 140% for glass B at pH<sub>RT</sub> 11/70°C (i.e.,  $1.04 \pm 1.45$  g m<sup>-2</sup> d<sup>-1</sup>).

### 3.3.2 | Case 3 (removal of dissolution rate and pH outliers)

The experimental outliers were excluded in Case 2 while Case 3 examines the removal of experimental outliers and dissolution rates obtained from tests where the pH<sub>RT</sub> was not controlled to within 0.3 pH units of the target pH<sub>RT</sub>. The Case 3 average dissolution rates reported with one standard deviation, average measured pH<sub>RT</sub> values with

**TABLE 4** Average dissolution rates at various pH (nominal and average measured) and temperature (nominal only) values from the interlaboratory study (ILS) study with data generated with 0.3 pH units of the target  $\text{pH}_{\text{RT}}$  (Case 3).

Glass ID	$\text{pH}_{\text{RT}}$	$T$ ( $^{\circ}\text{C}$ )	$N$	Measured	Average rate				
				$\text{pH}_{\text{RT}}$	( $\text{g m}^{-2} \text{d}^{-1}$ ) <sup>a</sup>	$s_r$	$R$	$s_R$	$R$
A	11	70	21	$10.9 \pm 0.1$	$2.37 \pm 0.79$	0.14	0.40	0.80	2.25
	10	70	18	$9.9 \pm 0.1$	$0.39 \pm 0.15$	0.01	0.04	0.15	0.42
	11	40	14	$10.9 \pm 0.1$	$0.27 \pm 0.05$	0.01	0.04	0.05	0.14
B	11	70	32	$10.8 \pm 0.1$	$1.18 \pm 0.47$	0.06	0.16	0.48	1.34
	10	70	19	$9.9 \pm 0.1$	$0.14 \pm 0.06$	0.01	0.02	0.06	0.17
	11	40	14	$10.9 \pm 0.1$	$0.12 \pm 0.02$	0.01	0.02	0.02	0.05
C	11	70	21	$10.9 \pm 0.1$	$1.63 \pm 0.40$	0.10	0.28	0.40	1.13
	10	70	18	$9.9 \pm 0.1$	$0.29 \pm 0.13$	0.01	0.03	0.13	0.36
	11	40	14	$10.9 \pm 0.1$	$0.15 \pm 0.02$	0.01	0.02	0.02	0.06
D	11	70	30	$10.9 \pm 0.1$	$3.57 \pm 0.97$	0.28	0.78	0.99	2.76
	10	70	20	$9.88 \pm 0.09$	$1.12 \pm 0.54$	0.05	0.14	0.56	1.56
	11	40	14	$10.9 \pm 0.1$	$0.36 \pm 0.04$	0.02	0.06	0.04	0.12

The  $N$ ,  $s_r$ ,  $r$ ,  $s_R$ , and  $R$  values for each condition are also provided.

<sup>a</sup>Uncertainty is presented as one standard deviation of all reported rate values considering the total number of tests performed ( $N$ ).

one standard deviation, and  $N$ ,  $s_r$ ,  $r$ ,  $s_R$ , and  $R$  values for each glass and condition excluding the outlier values are reported in Table 4. The  $\text{pH}_{\text{RT}}$  10/70 $^{\circ}\text{C}$  calculations for Case 3 are identical to Case 2 calculations (Table 3) as all the measured  $\text{pH}_{\text{RT}}$  values were within the  $\pm 0.3$  pH units of the target  $\text{pH}_{\text{RT}}$ , but values are included in Table 4 for completeness. For Case 3, test results obtained from 11 laboratories are included for the  $\text{pH}_{\text{RT}}$  10/70 $^{\circ}\text{C}$  calculations, 10 laboratories for  $\text{pH}_{\text{RT}}$  11/70 $^{\circ}\text{C}$ , and six laboratories for  $\text{pH}_{\text{RT}}$  11/40 $^{\circ}\text{C}$ , satisfying the minimum number of participating laboratories by the ASTM E691-23 for determining precision and bias.<sup>38</sup> The average rate increased for all glass/condition test combinations except the  $\text{pH}_{\text{RT}}$  10/70 $^{\circ}\text{C}$  tests as they were identical to the rates determined for Case 2. All excluded test results are attributed to the measured  $\text{pH}_{\text{RT}}$  values reported below the lower pH limit, emphasizing the influence of  $\text{pH}_{\text{RT}}$  on the dissolution rate.

The  $s_r$  values extend from 3% of the average rate (i.e.,  $0.40 \pm 0.01 \text{ g m}^{-2} \text{ d}^{-1}$  for Glass A at  $\text{pH}_{\text{RT}}$  10/70 $^{\circ}\text{C}$ ) to 8% of the average rate (i.e.,  $3.57 \pm 0.28 \text{ g m}^{-2} \text{ d}^{-1}$  for Glass D at  $\text{pH}_{\text{RT}}$  11/70 $^{\circ}\text{C}$ ). The corresponding  $r$  values vary from 10% for Glass A at  $\text{pH}_{\text{RT}}$  10/70 $^{\circ}\text{C}$  (i.e.,  $0.40 \pm 0.04 \text{ g m}^{-2} \text{ d}^{-1}$ ) to 20% for Glass D at  $\text{pH}_{\text{RT}}$  11/70 $^{\circ}\text{C}$  (i.e.,  $3.57 \pm 0.78 \text{ g m}^{-2} \text{ d}^{-1}$ ).

Meanwhile, the  $s_R$  values range from 10% of the average rate (i.e.,  $0.36 \pm 0.04 \text{ g m}^{-2} \text{ d}^{-1}$  for Glass D at  $\text{pH}_{\text{RT}}$  11/40 $^{\circ}\text{C}$ ) to 50% of the average rate (i.e.,  $1.12 \pm 0.56 \text{ g m}^{-2} \text{ d}^{-1}$  for Glass D at  $\text{pH}_{\text{RT}}$  10/70 $^{\circ}\text{C}$ ) with corresponding  $R$  values of 30% for Glass D at  $\text{pH}_{\text{RT}}$  11/40 $^{\circ}\text{C}$  (i.e.,  $0.36 \pm 0.12 \text{ g m}^{-2} \text{ d}^{-1}$ ) and 140% for Glass D at  $\text{pH}_{\text{RT}}$  10/70 $^{\circ}\text{C}$  (i.e.,  $1.12 \pm 1.56 \text{ g m}^{-2} \text{ d}^{-1}$ ).

The range for Case 3 for  $s_r$  values in comparison to average rates is smaller (i.e., 3%–8%) compared to the range observed for Case 2 (i.e., 3%–10%), indicating the repeatability slightly improves when a  $\pm 0.3$  pH unit tolerance is specified to the data set. The  $s_R$  values decreased from 20% to 50% of the average rate in Case 2 to 10%–50% in Case 3, indicating the reproducibility improved in Case 3, as well. However, multiple datapoints obtained for the  $\text{pH}_{\text{RT}}$  10/70 $^{\circ}\text{C}$  and  $\text{pH}_{\text{RT}}$  11/40 $^{\circ}\text{C}$  conditions were removed for Case 3, which may not be realistic for laboratories conducting this test in the future if the pH is difficult to control. Therefore, Case 4 and Case 5 were performed to limit the number of datapoints excluded by the pH tolerance while still addressing the effect of pH on the dissolution rate in the calculations.

### 3.3.3 | Case 5 (pH correction of dissolution rates with removal of dissolution rate outliers)

To those versed in the art, pH is known to be a relatively strong factor on the apparent dissolution rate of glasses, often causing rates to increase exponentially in the alkaline-pH range. Over a narrow range of pH ( $\sim 1$  pH unit), this increase in rate can be reasonably approximated by a linear trend. Accordingly, a linear function was fitted to the data to obtain a calculated variable rate as a function of  $\text{pH}_{\text{RT}}$  for Cases 4 and 5 to incorporate the test results outside of the  $\pm 0.3$  pH tolerance and thus evaluate the consistency of measured dissolution rates after accounting for the pH-dependence of glass dissolution rate. The linear function to calculate the variable rate is described by

**TABLE 5** Parameters  $a$  and  $b$  from the pH-rate function in Equation (2), calculated rates at target  $\text{pH}_{\text{RT}}$  (calculated target rate),  $N$ ,  $s_{\text{R}}$ , and  $R$  values for each condition are provided for Case 5.

Glass ID	$\text{pH}_{\text{RT}}$	$T$ ( $^{\circ}\text{C}$ )	$N$	pH-rate function parameters		Variable target rate ( $\text{g m}^{-2} \text{d}^{-1}$ )	$s_{\text{R}}$	$R$
				$a$	$b$			
A	11	70	25	1.99	-19.25	2.61	0.71	1.98
	10	70	18	0.76	-7.07	0.49	0.14	0.40
	11	40	22	0.12	-1.03	0.29	0.05	0.15
B	11	70	40	1.50	-15.16	1.34	0.37	1.05
	10	70	19	0.32	-3.02	0.18	0.06	0.17
	11	40	20	0.06	-0.51	0.12	0.02	0.05
C	11	70	25	0.94	-8.67	1.72	0.40	1.13
	10	70	18	0.71	-6.69	0.37	0.12	0.34
	11	40	20	0.04	-0.31	0.16	0.02	0.07
D	11	70	38	2.06	-18.95	3.72	0.97	2.71
	10	70	20	1.26	-11.36	1.28	0.55	1.55
	11	40	22	0.10	-0.74	0.38	0.05	0.15

Equation (2) as follows:

$$\text{variable rate} = a \times \text{pH}_{\text{RT}} + b \quad (2)$$

where coefficients  $a$  and  $b$  were fitted using Case 1 and Case 2 dissolution rates and corresponding  $\text{pH}_{\text{RT}}$  values for each glass/condition combination to generate calculated variable rates for Case 4 and Case 5, respectively.

The  $N$ ,  $a$ ,  $b$ ,  $s_{\text{R}}$ , and  $R$  values for Case 4 are given in Supporting Information Table 3, and the results for Case 5 are provided in Table 5. No  $s_{\text{r}}$  and  $r$  parameters are provided in Supporting Information Tables 3 and 5 for Case 4 and Case 5 as they are identical to the  $s_{\text{r}}$  and  $r$  parameters in Case 1 and Case 2, respectively. For each glass/condition combination, the variable rate at the target  $\text{pH}_{\text{RT}}$  (i.e., variable target rate) was larger than the average rates determined for Case 2 and Case 3, indicating the reduced pH effect (which caused the rates to be lower than expected) observed across the series had been accounted for.

The  $s_{\text{R}}$  values were determined in the same method as the other cases except measured rates were compared to variable rates determined using Equation (2) with the corresponding measured  $\text{pH}_{\text{RT}}$  rather than to the average of the measured rates. Therefore, the variable target rate is provided as a value to compare with the previous cases and the calculated  $s_{\text{R}}$  values.

In summary for Case 5, the  $s_{\text{R}}$  values range from 10% of the variable target rate (i.e.,  $0.38 \pm 0.05 \text{ g m}^{-2} \text{ d}^{-1}$  for glass D at  $\text{pH}_{\text{RT}} 11/40^{\circ}\text{C}$ ) to 40% of the variable target rate (i.e.,  $1.28 \pm 0.55 \text{ g m}^{-2} \text{ d}^{-1}$  for glass D at  $\text{pH}_{\text{RT}} 10/70^{\circ}\text{C}$ ) with corresponding  $R$  values of 40% for glass D at  $\text{pH}_{\text{RT}} 11/40^{\circ}\text{C}$  (i.e.,  $0.36 \pm 0.15 \text{ g m}^{-2} \text{ d}^{-1}$ ) and 120% for glass D at  $\text{pH}_{\text{RT}} 10/70^{\circ}\text{C}$  (i.e.,  $1.28 \pm 1.55 \text{ g m}^{-2} \text{ d}^{-1}$ ). The  $s_{\text{R}}$  values in comparison to the variable target rates decreased

from 20% to 50% of the average rate in Case 2 and 10%–50% in Case 3 to 10%–40% in Case 5, indicating the pH-rate correction approach improved the reproducibility more than Case 3.

### 3.3.4 | Summary of method precision and bias

In the present study, the recently developed SRCA test method is discussed in detail. The method can study the dissolution rate of glasses in forward-rate conditions at fixed pH and temperature. The method involves masking a section of the glass monolith with an inert material and, at the end of the test, measuring the difference between the height of the dissolved surface and the reference surface. The main advantage of the SRCA test method compared to previous test methods is the ability to measure several glass compositions simultaneously under highly dilute (low SA/V) conditions (that ostensibly approximate forward-rate behavior) without the need to perform a chemical assay of the solution or frequently replenish the contacting solution, as would be done in a flow-through method. This allows for a quick assessment of the relative durability of several glass specimens in parallel in a relatively short period of time without compromising the quality of the technical data. The SRCA method could also be applied to multiphase materials to examine the relative dissolution rate of the different phases in a material (e.g., glass-ceramics or cements).

The main disadvantage of the test method is the lack of information about the elemental release from a glass and extremely long durations required to gain information at low temperature and low pH combinations, or with very

**TABLE 6** Interlaboratory study (ILS) rates and the 95% reproducibility limits ( $R$ ) for the single-pass flow-through (SPFT) ILS and stirred-reactor coupon analysis (SRCA) ILS for Cases 2, 3, and 5 for low-activity reference material (LRM; Glass B in SRCA ILS) at  $\text{pH}_{\text{RT}} 11/70^\circ\text{C}$ .

	ILS rate $\pm R$ ( $\text{g m}^{-2} \text{d}^{-1}$ )
SPFT	$1.64 \pm 1.80$ (110%)
SRCA Case 2	$1.04 \pm 1.45$ (140%)
SRCA Case 3	$1.18 \pm 1.34$ (110%)
SRCA Case 5	$1.34 \pm 1.05$ (80%)

The percentage of  $R$  compared to the ILS rate is also provided.

durable glasses in a different composition regime. Tests are also conducted with an a priori assumption that the glass is dissolving at the forward rate. In other test methods, this can be assessed by evaluating the concurrent release of different glass components, or by running the test at multiple flow-rate-to-surface-area ratios to verify that the dissolution rate is invariant to changes in this ratio (i.e., the glass is dissolving at its maximum rate). If the glass is not dissolving at the forward rate, this may result in an alteration layer on the glass surface. Though further information about the glass alteration process can be examined if this were to happen, this would add another step to the analysis.

Five cases were considered to determine method precision and bias to account for experimental outliers and the pH-dependency on dissolution rates. The different cases, presented in Section 3.3, examine the effect of removing experimental outliers and correcting of the influence of pH on the glass dissolution rate. As expected, the precision and bias improved when experimental outliers were excluded and a correction to account for pH was used.

The results from the current study can be compared to a previous ILS conducted for ASTM C1662<sup>20</sup> to measure the precision of the dissolution rate measured by the SPFT method.<sup>47</sup> Table 6 provides LRM (Glass B in SRCA ILS) ILS rates at  $\text{pH}_{\text{RT}} 11/70^\circ\text{C}$  and 95% reproducibility limits ( $R$ ) from the SPFT ILS and from Cases 2, 3, and 5 from SRCA ILS. Regardless of the case used, the SRCA ILS rate is lower than the SPFT value although all values are within the 95% reproducibility limit of each other. The smallest  $R$  window occurs for the SRCA Case 5 (80%, i.e.,  $1.34 \pm 1.05 \text{ g m}^{-2} \text{d}^{-1}$ ) while SRCA Case 3 and SPFT have similar  $R$  windows (110% for each, respectively, i.e.,  $1.18 \pm 1.34 \text{ g m}^{-2} \text{d}^{-1}$  and  $1.04 \pm 1.45 \text{ g m}^{-2} \text{d}^{-1}$ ). Thus, when the pH control issues are addressed for SRCA either by a pH-corrected equation or by establishing a pH tolerance of 0.3 pH units, the SRCA method has greater or equal precision compared to the SPFT method.

## 4 | CONCLUSIONS

This work provides a thorough discussion on SRCA, detailing the test reactor, the impacts of variables such as sample polish and test duration, and the results of an ILS study involving twelve different institutions. The precision statement provided in Section 3.3.4 is for tests run in chemically buffered systems, although the SRCA method could be performed in different test solution such as relevant groundwaters. This novel method is efficient in assessing the relative durability of a wide range of glass compositions.

## ACKNOWLEDGMENTS

The authors would like to thank Jarrod Crum (PNNL) for his review of the manuscript. Funding for this work was provided by Washington River Protection Solutions. Pacific Northwest National Laboratory is a multiprogram national laboratory operated for the US Department of Energy by Battelle Memorial Institute under Contract DE-AC06-76RLO 1830. We thank Alexander Westesen and James Davis for assembling the SRCA reactor parts list and CAD drawings. John S. McCloy thanks D. Bollinger, J. Bussey, J. Sly, and R. Antonio for assistance with the tests. Yuta Takahashi, Seiichiro Mitsui, and Junya Sato thank Dr. T. Osugi for his kind arrangements on JAEA's participation. Mike T. Harrison would like to thank T. Taylor and K. Summers for assistance with the tests. Karine Ferrand thanks Pieter Schroeders and Ben Gielen for assistance with the tests. Corning participants would like to thank Hugh McMahon for assistance with the tests.

## CONFLICT OF INTEREST STATEMENT

The authors declare no conflicts of interest.

## DATA AVAILABILITY STATEMENT

The raw data and the processed data required to reproduce these findings are available to download from the supporting information available with this article.

## ORCID

Joelle T. Reiser  <https://orcid.org/0000-0002-2638-1580>

Benjamin Parruzot  <https://orcid.org/0000-0002-2841-6660>

Stéphane Gin  <https://orcid.org/0000-0002-1950-9195>

Nicholas J. Smith  <https://orcid.org/0000-0002-8726-9525>

Jincheng Du  <https://orcid.org/0000-0003-4805-7498>

John S. McCloy  <https://orcid.org/0000-0001-7476-7771>

## REFERENCES

- Jantzen CM, Brown KG, Pickett JB. Durable glass for thousands of years. *Int J Appl Glass Sci*. 2010;1:38–62.

2. Grambow B. Nuclear waste glasses—how durable?. *Elements*. 2006;2:357–64.
3. Marcial J, Riley BJ, Kruger AA, Lonergan CE, Vienna JD. Hanford low-activity waste vitrification: a review. *J Hazard Mater*. 2024;461:132437.
4. Neeway JJ, Rieke PC, Parruzot BP, Ryan JV, Asmussen RM. The dissolution behavior of borosilicate glasses in far-from equilibrium conditions. *Geochim Cosmochim Acta*. 2018;226:132–48.
5. Vienna JD, Neeway JJ, Ryan JV, Kerisit SN. Impacts of glass composition, pH, and temperature on glass forward dissolution rate. *NPJ Mater Degrad*. 2018;2:22.
6. Pierce EM, Rodriguez EA, Calligan LJ, Shaw WJ, McGrail BP. An experimental study of the dissolution rates of simulated aluminoborosilicate waste glasses as a function of pH and temperature under dilute conditions. *Appl Geochem*. 2008;23:2559–73.
7. McGrail BP, Ebert WL, Bakel AJ, Peeler DK. Measurement of kinetic rate law parameters on a Na-Ca-Al borosilicate glass for low-activity waste. *J Nucl Mater*. 1997;249:175–89.
8. Backhouse DJ, Fisher AJ, Neeway JJ, Corkhill CL, Hyatt NC, Hand RJ. Corrosion of the International Simple Glass under acidic to hyperalkaline conditions. *NPJ Mater Degrad*. 2018;2:29.
9. Cassingham N, Corkhill C, Backhouse D, Hand RJ, Ryan JV, Vienna JD, et al. The initial dissolution rates of simulated UK magnox-ThORP blend nuclear waste glass as a function of pH, temperature and waste loading. *Mineral Mag*. 2015;79:1529–42.
10. Abraitis PK, Livens FR, Monteith JE, Small JS, Trivedi DP, Vaughan DJ, et al. The kinetics and mechanisms of simulated British Magnox Waste glass dissolution as a function of pH, silicic acid activity, and time in low temperature aqueous systems. *Appl Geochem*. 2000;15:1399–416.
11. Jollivet P, Gin S, Schumacher S. Forward dissolution rate of silicate glasses of nuclear interest in clay-equilibrated groundwater. *Chem Geol*. 2012;330–331:207–17.
12. Thorpe CL, Neeway JJ, Pearce CI, Hand RJ, Fisher AJ, Walling SA, et al. Forty years of durability assessment of nuclear waste glass by standard methods. *NPJ Mater Degrad*. 2021;5:61.
13. Pierce EM, Richards EL, Davis AM, Reed LR, Rodriguez EA. Aluminoborosilicate waste glass dissolution under alkaline conditions at 40°C: implications for a chemical affinity-based rate equation. *Environ Chem*. 2008;5:73.
14. Icenhower JP, McGrail BP, Shaw WJ, Pierce EM, Nachimuthu P, Shuh DK, et al. Experimentally determined dissolution kinetics of Na-rich borosilicate glass at far from equilibrium conditions: implications for transition state theory. *Geochim Cosmochim Acta*. 2008;72:2767–88.
15. Icenhower JP, Steefel CI. Experimentally determined dissolution kinetics of SON68 glass at 90°C over a silica saturation interval: evidence against a linear rate law. *J Nucl Mater*. 2013;439:137–47.
16. Icenhower JP, Steefel CI. Dissolution rate of borosilicate glass SON68: a method of quantification based upon interferometry and implications for experimental and natural weathering rates of glass. *Geochim Cosmochim Acta*. 2015;157:147–63.
17. Gudbrandsson S, Wolff-Boenisch D, Gislason SR, Oelkers EH. Experimental determination of plagioclase dissolution rates as a function of its composition and pH at 22°C. *Geochim Cosmochim Acta*. 2014;139:154–72.
18. Hamilton JP, Pantano CG, Brantley SL. Dissolution of albite glass and crystal. *Geochim Cosmochim Acta*. 2000;64:2603–15.
19. Pierce EM, Reed LR, Shaw WJ, McGrail BP, Icenhower JP, Windisch CF, et al. Experimental determination of the effect of the ratio of B/Al on glass dissolution along the nepheline (NaAlSiO<sub>4</sub>)-malinkoite (NaBSiO<sub>4</sub>) join. *Geochim Cosmochim Acta*. 2010;74:2634–54.
20. ASTM International (2024). C1662-24 standard practice for measurement of the glass dissolution rate using the single-pass flow-through test method. West Conshohocken, PA.
21. Inagaki Y, Kikunaga T, Idemitsu K, Arima T. Initial dissolution rate of the International Simple Glass as a function of pH and temperature measured using microchannel flow-through test method. *Int J Appl Glass Sci*. 2013;4:317–27.
22. Inagaki Y, Makigaki H, Idemitsu K, Arima T, Mitsui S, Noshita K. Initial dissolution rate of a Japanese high-level waste glass P0798 as a function of pH and temperature measured by using micro-channel flow-through test method. *J Nucl Sci Technol*. 2012;49:438–49.
23. Delage F, Dussossoy JL. R7T7 glass initial dissolution rate measurements using a high-temperature Soxhlet device. *Mater Res Soc Symp Proc*. 1991;212:41–48.
24. Guo R, Brigden CT, Gin S, Swanton SW, Farnan I. The effect of magnesium on the local structure and initial dissolution rate of simplified UK Magnox waste glasses. *J Non-Cryst Solids*. 2018;497:82–92.
25. ASTM International (2021). C1220-21 standard test method for static leaching of monolithic waste forms for disposal of radioactive waste. West Conshohocken, PA.
26. Icenhower JP, Lutge A, McGrail BP, Beig MS, Arvidson RS, Rodriguez EA, et al. Results of vertical scanning interferometry (VSI) of dissolved borosilicate glass: evidence for variable surface features and global surface retreat. *Mater Res Soc Symp Proc*. 2003;757:II.5.1.
27. Wild B, Imfeld G, Daval D. Direct measurement of fungal contribution to silicate weathering rates in soil. *Geology*. 2021;49:1055–58.
28. Fischer C, Lutge A. Converged surface roughness parameters—a new tool to quantify rock surface morphology and reactivity alteration. *Am J Sci*. 2007;307:955–73.
29. Noiriel C, Oursin M, Daval D. Examination of crystal dissolution in 3D: a way to reconcile dissolution rates in the laboratory? *Geochim Cosmochim Acta*. 2020;273:1–25.
30. Kumar A, Reed J, Sant G. Vertical scanning interferometry: a new method to measure the dissolution dynamics of cementitious minerals. *J Am Ceram Soc*. 2013;96:2766–78.
31. Mascarin L, Valentini L, Artioli G, Dalconi MC, Colombani J. Dissolution-precipitation kinetics during C3S hydration: a holographic interferometry study. *Cem Concr Res*. 2023;173:107252.
32. Garg N, Skibsted J. Dissolution kinetics of calcined kaolinite and montmorillonite in alkaline conditions: evidence for reactive Al(V) sites. *J Am Ceram Soc*. 2019;102:7720–34.
33. Crum JV, Neeway JJ, Riley BJ, Zhu Z, Olszta MJ, Tang M. Dilute condition corrosion behavior of glass-ceramic waste form. *J Nucl Mater*. 2016;482:1–11.
34. ASTM International. (2022) D7778-15(2022)e1 standard guide for conducting an interlaboratory study to determine the precision of a test method. West Conshohocken, PA.
35. Uhl VW, Gray JB. *Mixing: theory and practice*, Volume . Academic Press, New York; 1966.

36. ASTM International. (2024) C1926-24 Standard test method for measurement of glass dissolution rate using stirred dilute reactor conditions on monolithic samples. West Conshohocken, PA.
37. ASTM International. (2024). D1193-24 Standard specification for reagent water. West Conshohocken, PA.
38. ASTM International. (2023) E691-23 standard practice for conducting an interlaboratory study to determine the precision of a test method. West Conshohocken, PA.
39. Muller IS, Diener G, Joseph I, Pegg IL. Proposed approach for development of LAW glass formulation correlation. VSL-04L4460-1 and ORP-56326. Washington, D.C.: Vitreous State Laboratory, The Catholic University of America; 2004.
40. Pierce EM, McGrail BP, Rodriguez EA, Schaef HT, Saripalli KP, Serne RJ, et al. Waste form release data package for the 2005 integrated disposal facility performance assessment. PNNL-14805. Richland, WA, USA: Pacific Northwest National Laboratory; 2004.
41. Ebert WL, Wolf SF. An intralaboratory study of a standard glass for acceptance testing of low activity waste glass. *J Nucl Mater.* 2000;282:112–24.
42. Ryan JV, Smith NJ, Neeway JJ, Reiser JT, Parruzot B, Tietje S, et al. ISG-2: properties of the second International Simple Glass. *NPJ Mater Degrad.* 2023;7:47.
43. Crum JV, Kissinger RM, Cooley SK, Silverstein JA, Vienna JD, Kim DS, et al. Low-activity waste glass standards preparation and characterization for calibration of analytical instruments. PNNL-31372. Richland, WA, USA: Pacific Northwest National Laboratory; 2021.
44. Vienna JD, Heredia-Langner A, Cooley SK, Holmes AE, Kim DS, Lumetta NA. Glass property-composition models for support of Hanford WTP LAW facility operation. PNNL-30932 Rev. 2. Richland, WA: Pacific Northwest National Laboratory; 2022.
45. Crum JV, Reiser JT, Parruzot B, Neeway JJ, Kerisit SN, Cooley SK, et al. Seeded stage III glass dissolution behavior of a statistically designed glass matrix. *J Am Ceram Soc.* 2021;104:4145–62.
46. Ryan JV, Cooley SK, Parruzot BP, Reiser JT, Corkhill CL, Du J, et al. Stirred-reactor coupon analysis: an international round robin study. PNNL-33141. Richland, WA: Pacific Northwest National Laboratory; 2022.
47. Ebert WL. Interlaboratory study of the reproducibility of the single-pass flow-through test method: measuring the dissolution rate of LRM glass at 70°C and pH 10. ANL-05/33. Argonne, IL, USA: Argonne National Laboratory; 2005.

## SUPPORTING INFORMATION

Additional supporting information can be found online in the Supporting Information section at the end of this article.

**How to cite this article:** Reiser JT, Neeway JJ, Cooley SK, Parruzot B, Heredia-Langner A, Gin S, et al. The development and application of the stirred-reactor coupon analysis (SRCA) test method. *Int J Appl Glass Sci.* 2025;e16707.  
<https://doi.org/10.1111/ijag.16707>